E4F1-mediated control of pyruvate dehydrogenase activity is essential for skin homeostasis

Perrine Goguet-Rubio, Berfin Seyran, Laurie Gayte, Florence F. Bernex, Anne Sutter, Hélène Delpech, Laetitia Karine Linares, Romain Riscal, Cendrine Repond, Genevieve Rodier, et al.

E4F1-mediated control of pyruvate dehydrogenase activity is essential for skin homeostasis

Perrine Goguet-Rubio[a,b,c,d,e,1], Berfin Seyran[a,b,c,d,e,1], Laurie Gayte[a,b,c,d,e], Florence Bernex[a,c,f], Anne Sutter[a,b,c,d,e], Hélène Delpech[a,b,c,d,e,g], Laetitia Karine Linares[a,b,c,d,e], Romain Riscal[a,b,c,d,e], Cendrine Repond[h], Geneviève Rodier[a,b,c,d,e,g], Olivier Kirsh[g,i], Jawida Touhami[c,g], Jean Noel[a,b,c,d,f], Charles Vincent[a,b,c,d], Nelly Pirot[a,b,c,d,f], Guillaume Pavlovic[j], Yann Herault[j], Marc Sitbon[c,g], Luc Pellerin[h], Claude Sardet[a,b,c,d,e,g], Matthieu Lacroix[a,b,c,d,e,2,3], and Laurent Le Cam[a,b,c,d,e,2,3]

[a]Institut de Recherche en Cancérologie de Montpellier, Montpellier F-34298, France; [b]INSERM U1194, Montpellier F-34298, France; [c]University of Montpellier, Montpellier F-34090, France; [d]Institut Régional du Cancer de Montpellier, Montpellier F-34298, France; [e]Equipe labellisée Ligue Contre le Cancer, 75013 Paris, France; [f]Réseau d'Histologie Expérimentale de Montpellier, BioCampus, CNRS-UMS3426, F-34094 Montpellier, France; [g]Institut de Génétique Moléculaire de Montpellier, CNRS-UMR5535, Montpellier 34293, France; [h]Department of Physiology, University of Lausanne, 1005 Lausanne, Switzerland; [i]Epigenetics and Cell Fate, University Paris Diderot, Sorbonne Paris Cite, UMR7216 CNRS, Paris 75013, France; and [j]Institut de la Clinique de la Souris-Mouse Clinical Institute, PHENOMIN, CNRS-UMR7104, INSERM U964, Université de Strasbourg, Illkirch, France

Edited by Steven L. McKnight, The University of Texas Southwestern Medical Center, Dallas, TX, and approved August 5, 2016 (received for review February 18, 2016)

The multifunctional protein E4 transcription factor 1 (E4F1) is an essential regulator of epidermal stem cell (ESC) maintenance. Here, we found that E4F1 transcriptionally regulates a metabolic program involved in pyruvate metabolism that is required to maintain skin homeostasis. E4F1 deficiency in basal keratinocytes resulted in deregulated expression of *dihydrolipoamide acetyltransferase* (*Dlat*), a gene encoding the E2 subunit of the mitochondrial pyruvate dehydrogenase (PDH) complex. Accordingly, *E4f1* knock-out (KO) keratinocytes exhibited impaired PDH activity and a redirection of the glycolytic flux toward lactate production. The metabolic reprogramming of *E4f1* KO keratinocytes associated with remodeling of their microenvironment and alterations of the basement membrane, led to ESC mislocalization and exhaustion of the ESC pool. ShRNA-mediated depletion of *Dlat* in primary keratinocytes recapitulated defects observed upon *E4f1* inactivation, including increased lactate secretion, enhanced activity of extracellular matrix remodeling enzymes, and impaired clonogenic potential. Altogether, our data reveal a central role for *Dlat* in the metabolic program regulated by E4F1 in basal keratinocytes and illustrate the importance of PDH activity in skin homeostasis.

E4F1 | PDH | pyruvate | skin | stem cell

Renewal and wound healing of the epidermis rely on a pool of epidermal stem cells (ESC) located in the basal layer of the interfollicular epithelium (IFE) and in the bulge region of the hair follicle (HF). In the IFE, these long-lived ESC give rise to progenitors with increased proliferative capacities that differentiate into keratinocytes as they migrate upward into suprabasal layers. Numerous studies have addressed the role of several key signaling pathways, such as those implicating bone morphogenetic proteins, TGF-β, Notch, Sonic Hedgehog, or Wnt in skin homeostasis, and how they control ESC maintenance (1–3). The role of these pathways in regulating stemness has been attributed to the regulation of cell proliferation, cell death, cellular senescence, cell adhesion, or differentiation. Although previous data indicate that some of these stem cell regulators also control energy metabolism in the hematopoietic or neuronal lineages (4), very few studies have yet addressed their metabolic functions in keratinocytes. In addition, the potential role of specific metabolic regulators in the control of skin homeostasis remains poorly documented. Nevertheless, previous observations indicate that deregulation of the nutrient-sensing mammalian target of rapamycin pathway in basal keratinocytes occurs as a consequence of prolonged Wnt signaling, leading to the progressive exhaustion of HF bulge stem cells (5). Recent data also indicate that genetic inactivation in mouse epidermis of *mitochondrial transcription factor A* (*Tfam*), a gene involved in mitochondrial DNA replication and transcription, impinges on keratinocyte differentiation but does not impair maintenance of basal keratinocytes (6). Although these results suggest that basal keratinocytes display a metabolic status that is different from their differentiated counterparts, further studies are warranted to decipher the poorly understood role of metabolism in the regulation of epidermal cell fate.

We previously identified the multifunctional protein E4 transcription factor 1 (E4F1) as an essential regulator of skin homeostasis and ESC maintenance (7). E4F1 was originally identified as a cellular target of the E1A viral oncoprotein (8, 9). Since then, several laboratories have shown that E4F1 directly interacts with several oncogenes and tumor suppressors, including p53, BMI1, RB, RASSF1A, SMAD4, or HMGA2 proteins (10–16). Consistent with its implication in different oncogenic pathways, E4F1 acts as a survival factor in cancer cells (17, 18). Moreover, characterization of *E4f1* knock-out (KO) mice showed that *E4f1* is an essential gene in embryonic stem cells and during early embryogenesis (19). Using *E4f1* conditional KO mice, we previously reported that *E4f1*

Significance

We found that the multifunctional protein E4 transcription factor 1 (E4F1) transcriptionally regulates a metabolic program involved in pyruvate metabolism that is required to maintain skin homeostasis. E4F1 deficiency in skin resulted in deregulated expression of *dihydrolipoamide acetlytransferase* (*Dlat*), a gene encoding the E2 subunit of the mitochondrial pyruvate dehydrogenase (PDH) complex. Accordingly, *E4f1* knock-out (KO) keratinocytes exhibited impaired PDH activity and a metabolic reprogramming associated with remodeling of their microenvironment and alterations of the basement membrane, leading to epidermal stem cell mislocalization and exhaustion of the epidermal stem cell pool. Our data reveal a central role for *Dlat* in the metabolic program regulated by E4F1 in skin and illustrate the importance of PDH activity in skin homeostasis.

Author contributions: M.S., L.P., C.S., M.L., and L.L.C. designed research; P.G.-R., B.S., L.G., A.S., H.D., L.K.L., R.R., C.R., G.R., O.K., J.T., J.N., C.V., N.P., and M.L. performed research; G.P., Y.H., and M.S. contributed new reagents/analytic tools; F.B., M.L., and L.L.C. analyzed data; and M.L. and L.L.C. wrote the paper.

The authors declare no conflict of interest.

This article is a PNAS Direct Submission.

[1]P.G.-R. and B.S. contributed equally to this work.

[2]M.L. and L.L.C. contributed equally to this work.

[3]To whom correspondence may be addressed. Email: matthieu.lacroix@inserm.fr or laurent.lecam@inserm.fr.

This article contains supporting information online at www.pnas.org/lookup/suppl/doi:10.1073/pnas.1602751113/-/DCSupplemental.

 www.pnas.org/cgi/doi/10.1073/pnas.1602751113

inactivation in the epidermis results in ESC defects through a mechanism that involves, at least partly, the deregulation of the Bmi1–Arf–p53 pathway (7). Here, we show evidence supporting a major role for E4F1 in pyruvate metabolism that governs ESC maintenance and skin homeostasis.

Results

_E4f1_ Inactivation in Basal but Not Suprabasal Adult Keratinocytes Leads to Epidermal Defects and Exhaustion of the ESC Pool. Using *E4f1* whole-body conditional KO mice (*E4f1KO; RERT*), we previously identified an essential role for *E4f1* in adult skin homeostasis (7). In this genetically engineered mouse model, *E4f1* inactivation was achieved in the entire skin of adult animals, including the dermal compartment. To assess the cell of origin of these skin defects, we generated new mouse strains by crossing *E4f1* conditional KO mice to transgenic animals expressing the tamoxifen (tam) -inducible CreER recombinase under the control of the keratin 14 (K14) or keratin 10 (K10) promoters [hereafter referred to as *E4f1*(*K14*)KO and *E4f1*(*K10*)KO strains], allowing acute inactivation of *E4f1* in adult keratinocytes of the basal or spinous layers, respectively (20).

Molecular and histological analyses of adult back skin of 8- to 12-wk-old *E4f1*(*K10*)KO animals confirmed that topical skin applications of tam activated the Cre recombinase in suprabasal but not in basal keratinocytes (Fig. S1). Neither histological alterations nor differences in the expression pattern of the basal-cell specific K14 marker and of the differentiation markers K10 and involucrin were identified in skin samples harvested up to 4 mo upon regular tam administration (Fig. S2). In sharp contrast, inactivation of *E4f1* in adult basal keratinocytes of *E4f1(K14)KO* mice resulted in skin phenotypes that recapitulated those originally observed in tam-treated *E4f1*$^{-/flox}$; *RERT* adult mice. Thus, 2 wk after tam administration, *E4f1*(*K14*)KO mice displayed epidermal hyperplasia (acanthosis), altered differentiation (dyskeratosis), and a thicker and parakeratotic cornified layer (Fig. 1*A* and Fig. S3). Aberrant hyperproliferation and mislocalisation of basal keratinocytes was evidenced in *E4f1*-deficient epidermis by increased *K*i67 staining, the presence of K14$^+$ cells in suprabasal layers, and the expression of keratin 6 (K6) in the IFE (Fig. S4). At later time points (4–5 wk after tam administration), *E4f1*-deficient epidermis then became hypocellular, whereas the hyperkeratosis remained evident (Fig. 1*A*). In addition, impaired keratinocyte differentiation was illustrated by aberrant expression of K10 and involucrin (Fig. S4).

Consistent with our previous observations, ablation of *E4f1* in adult basal keratinocytes altered ESC function and resulted in the definitive exhaustion of the ESC pool. Indeed, tam administration to *E4f1*(*K14*)*KO* mice led to the loss of expression of the bulge HF stem cell marker keratin 15 (K15) (Fig. 1*B*). Flow cytometry analysis of HF stem cells identified by the coexpression of CD34 and high levels of α6-integrin (CD34$^+$/α6^{high}) confirmed that tam-treated *E4f1*(*K14*)KO adult epidermis contained fewer HF stem cells compared with control epidermis (0.65% ± 0.15 vs. 2.25% ± 0.4) (Fig. 1*C*). We also tracked ESCs in the IFE by analyzing the number of label retaining cells (LRCs) using an adaptation of an in vivo labeling protocol of multipotent ESC based on the utilization of the nucleotide analog ethynyl-2′-deoxyribose (EdU) (21). These analyses showed that *E4f1* inactivation resulted in a significant decrease in the number of LRCs 5 wk after tam administration, indicating that *E4f1* deficiency led to the definitive loss of ESC in vivo (Fig. 1*D*). Finally, *E4f1*KO ESC defects were also illustrated ex-vivo by their impaired clonogenic potential (Fig. 1*E*).

Thus, these data demonstrate that the epidermal hyperplasia, hyperkeratosis, differentiation defects, and exhaustion of the ESC pool of E4F1-deficient epidermis originate from alterations in basal rather than suprabasal keratinocytes.

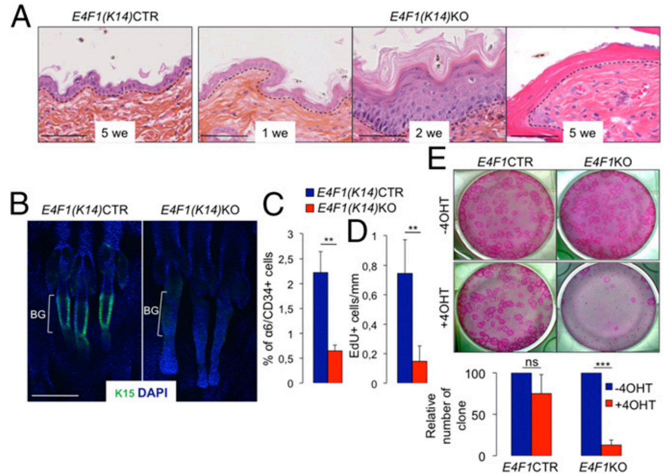

Fig. 1. E4F1 deficiency in basal keratinocytes leads to skin defects and exhaustion of the ESC pool. (*A*) Microphotographs of (HES)-stained skin sections prepared from *E4F1*(*K14*)KO mice or *E4F1*(*K14*)CTR littermates, 1, 2, or 5 wk after tam administration. Dashed lines indicate the separation between the epidermis and the dermis. (Scale bars, 100 μm.) (*B*) Whole mounts of tail epidermis prepared from adult *E4F1*(*K14*)KO and CTR mice, 5 wk after tam application, stained with K15 antibody and DAPI. Brackets: bulge area (BG) of the HF. (Scale bar, 100 μm.) (*C*) Number of follicular stem cells (FSC) in back skin epidermis prepared from the same mice as in *B*. FACS-analysis of α6/CD34 CD34^{high} FSC in back skin epidermis prepared from the same mice as in *B* (mean ± SEM; $n = 10$). (*D*) Number of label-retaining (EdU$^+$) interfollicular stem cells (LRCs) detected by immunofluorescence (IF) on back-skin sections prepared from adult *E4F1*(*K14*)KO mice or *E4F1*(*K14*)CTR littermates, 5 wk after tam application. Histobars represent the mean value ± SEM of EdU$^+$ cells per millimeter of epidermis ($n = 5$ animals per group). (*E*) Clonogenic assays performed with *E4F1KO* and CTRL primary murine keratinocytes cultured in presence or absence of 4OHT, as indicated ($n = 5$). Histobars represent the total number of clones per well relative to control cells (expressed as percentages) determined after rhodamine B staining. ***$P < 0.001$; **$P < 0.01$; ns, not significant.

E4F1 Controls Pyruvate Metabolism in Keratinocytes Through Transcriptional Regulation of the E2 Subunit of the Pyruvate Dehydrogenase Complex _Dlat_. Using a pan-genome ChIP approach combined with next-generation sequencing (ChIP-seq), we identified E4F1 binding sites at the whole-genome level in primary mouse embryonic fibroblasts and embryonic stem cells (18, 22). Functional annotation of E4F1 direct target genes indicated a significant enrichment in genes implicated in metabolism, including a set of five genes encoding core components or regulators of the mitochondrial pyruvate dehydrogenase (PDH) complex (PDC), a multimeric complex that converts pyruvate into Acetyl-CoA (AcCoA). In embryonic stem cells, this set of E4F1-controlled genes includes the E2 and E3 subunits of the PDC, *dihydrolipoamide acetyltransferase* (*Dlat*) and *dihydrolipoyl dehydrogenase* (*Dld*), the regulatory subunit of the PDH phosphatase complex (*Pdpr*), the pyruvate transporter of the inner mitochondrial membrane *Brp44l*/*Mpc1* (23, 24), and the mitochondrial transporter *Slc25a19* that transports the PDH cofactor thiamine pyrophosphate (25). These results prompted us to evaluate whether E4F1 also controlled this set of PDH-related genes in primary keratinocytes. First, we confirmed by quantitative ChIP that endogenous E4F1 was recruited to the promoter of *Dlat*, *Dld*, *Slc25a19*, and *Brp44l* in cultured primary murine keratinocytes (Fig. 2*A*). Similarly to *E4f1*KO fibroblasts and muscle cells, E4F1-deficient keratinocytes displayed a marked decrease of *Dlat* mRNA level. However, the expression of *Dld*, *Pdpr*, *Slc25a19*, and *Brp44l*/*Mpc1* remained unchanged upon *E4f1* inactivation, suggesting that other E4F1-independent mechanisms contribute to their expression in keratinocytes (Fig. 2*B*). The mRNA levels of other PDH-related genes, including *Pdha1*, which encodes the E1

PHYSIOLOGY

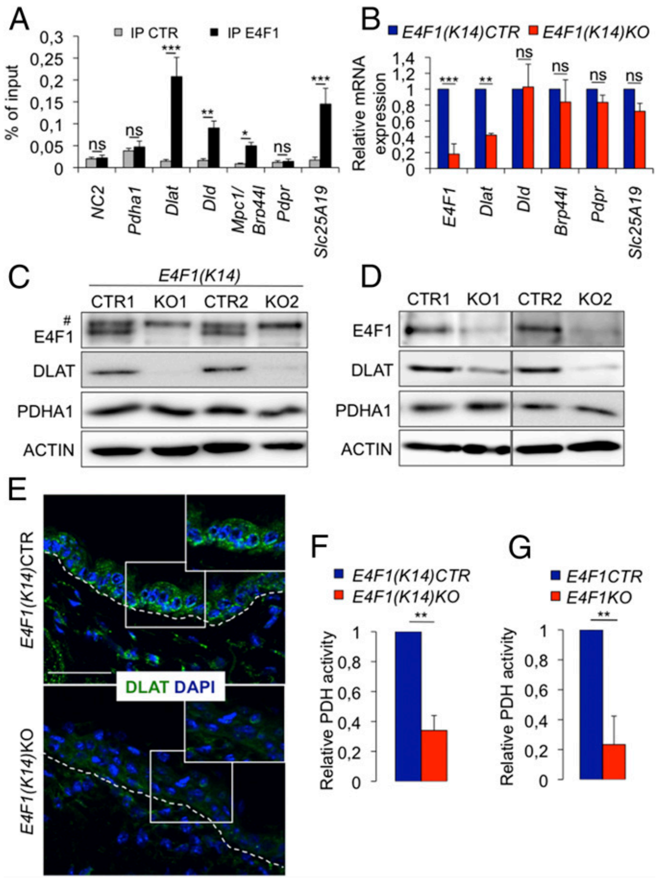

Fig. 2. *E4f1* inactivation in basal keratinocytes results in decreased *Dlat* expression and impaired PDH activity. (*A*) ChIP-qPCR assays performed with anti-E4F1 or control (CTR) antibodies in cultured primary keratinocytes on the promoter region of *Dlat*, *Dld*, *Mpc1/brp44l*, *Pdpr*, and *Slc25a19*. A gene-poor noncoding region of chromosome 6 (NC2) and the *Pdha1* promoter region (TSS, transcription start site) were used as controls. Enrichments are represented as percentages of input **(**mean value ± SEM; $n = 3$). (*B*) mRNA levels of *E4f1*, *Dlat*, *Dld*, *Brp44L/Mpc1*, *Pdpr* and *Slc25a19* in the epidermis of *E4f1(K14)*KO mice or *E4f1(K14)*CTR littermates, 1 wk after tam administration. Histobars represent the mean value ± SEM ($n = 5$) determined by RT-qPCR. (*C* and *D*) Protein levels of E4F1, DLAT, PDHA1, and β-actin (loading control) determined by immunoblotting in (*C*) total protein extracts prepared from epidermis of *E4f1(K14)*KO mice and control littermates, 1 wk after tam administration, or (*D*) *E4f1KO* or CTRL cultured primary keratinocytes. #Non-specific band. (*E*) Immunostaining of DLAT in skin sections prepared from the same mice as in *C*. Sections were counterstained with DAPI. (Scale bar, 50 μm.) (*F* and *G*) PDH activity measured in protein extracts prepared (*F*) from epidermis of *E4f1(K14)*KO and CTR mice, 1 wk after tam administration, or (*G*) from cultured primary keratinocytes of the indicated genotype using Colorimetric Assay kit (Biovision) (mean ± SEM, $n = 5$). All analyses in cultured primary keratinocytes were performed after 4 d of culture in the presence of 4OHT. ***$P < 0.001$; **$P < 0.01$; *$P < 0.05$; ns, not significant.

subunit of the PDC, the PDH -kinases 1/4 (*Pdk*1, *Pdk4*) and -phosphatases 1/2 (*Pdp1*, *Pdp2*) remained unchanged in *E4f1*-deficient keratinocytes (Fig. S5). Decreased *Dlat* expression was confirmed at the protein level, as shown by immunostaining of skin samples prepared from *E4f1*(*K14*)KO animals, 1 wk after tam-administration. This decrease was further confirmed by immunoblotting both in tam-treated *E4f1*(*K14*)KO epidermis and in cultured *E4f1*KO primary keratinocytes (Fig. 2 *C–E*). Consistent with DLAT deregulation, altered PDH enzymatic activity was detected in these cells (Fig. 2 *F* and *G* and Fig. S6*A*). Taken together, these data indicate that the E2 subunit of the PDC *Dlat* is a major direct transcriptional target of E4F1 in basal keratinocytes.

***E4f1KO* Results in Metabolic Reprogramming of Keratinocytes.** Next, we characterized the metabolic consequences of impaired PDH activity in E4F1-deficient keratinocytes. We postulated that decreased PDH activity in E4F1-deficient keratinocytes triggered a decrease of glucose-derived AcCoA production and the redirection of the glycolytic flux toward lactate production (Fig. 3*A*). Consistent with this hypothesis and the role of AcCoA as a donor substrate for acetylation reactions, *E4f1*KO keratinocytes exhibited decreased histone H4 acetylation, as shown by immunoblotting using an anti-pan-acetyl lysine histone H4 antibody (Fig. 3*B*). Moreover, in line with increased pyruvate metabolism by the NADH-dependent lactate dehydrogenase (LDH), *E4f1*KO keratinocytes displayed an increased NAD^+/NADH ratio (Fig. 3*C*). Increased expression of the glucose transporter GLUT1 suggested that glucose uptake increased upon *E4f1* inactivation in keratinocytes (Fig. S6*B*). These cells also exhibited increased expression of the monocarboxylate transporter MCT4 that favors the efflux of lactate outside the cell (Fig. 3 *D* and *E*). Accordingly, increased lactate secretion by *E4f1*KO keratinocytes was evidenced by a change in their extracellular acidification rate (ECAR) (Fig. 3*F*). Other metabolic changes were observed in E4F1-deficient keratinocytes, as illustrated by increased fatty acid oxidation (FAO) (Fig. 3*G*). This adaptative metabolic response was likely sufficient to sustain mitochondrial respiration because no significant difference was observed in oxygen consumption upon *E4f1* inactivation in keratinocytes cultured in complete medium (Fig. S6*D*). Analyses of tam-treated *E4f1*(K14)KO mice and control littermates confirmed that E4F1-deficient keratinocytes underwent the same metabolic

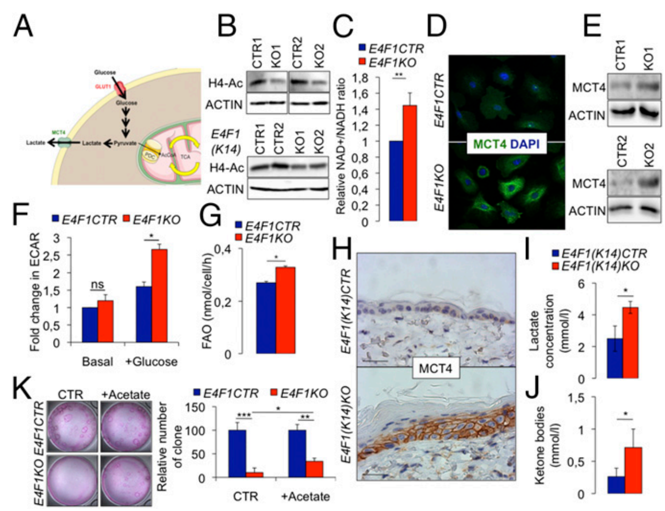

Fig. 3. Metabolic reprogramming of E4F1-deficient keratinocytes. (*A*) Schematic representation of the metabolic reprogramming in *E4f1KO* keratinocytes including the redirection of the glycolytic flux toward lactate production. (*B*) Protein levels of acetylated-lysine histone H4 and β-actin (loading control) determined by immunoblotting in total protein extracts prepared from epidermis of *E4f1(K14)*KO mice (*Upper*) or from *E4f1KO* cultured primary keratinocytes (*Lower*) and match control (CTR) samples. (*C*) NAD^+/NADH ratio in *E4f1KO* and CTR cultured primary keratinocytes (mean ± SEM; $n = 9$). (*D* and *E*) MCT4 expression was determined by IF (*D*) and by immunoblotting (*E*) in *E4f1KO* and CTR cultured primary keratinocytes. (Magnification: 40×.) (*F*) ECAR of *E4f1KO* and CTR primary keratinocytes in basal conditions or after addition of glucose (mean ± SEM; $n = 5$). (*G*) Relative level of FAO measured upon incubation of *E4f1KO* and CTR cultured keratinocytes with ^{3}H-palmitate (mean ± SEM of $n = 5$). (*H*) Immunohistochemistry analysis of MCT4 expression in skin sections prepared from *E4f1(K14)*KO and CTR mice, 2 wk after 4OHT administration. (Scale bar, 50 μm.) (*I* and *J*) Lactate (*I*) and ketone bodies (*J*) levels in the serum of *E4f1 (K14)*KO mice and CTR littermates, 1 wk after tam administration ($n = 5$ animals per group). (*K*) Clonogenic assays performed with *E4f1KO* and CTR primary keratinocytes in presence or absence or acetate, as indicated ($n = 3$). ***$P < 0.001$; **$P < 0.01$; *$P < 0.05$; ns, not significant. TCA, tricarboxylic acid cycle.

reprogramming in vivo. Thus, immunohistochemistry (IHC) analyses of skin samples prepared from these animals indicated that *E4f1* inactivation in basal keratinocytes resulted in increased expression of GLUT1, MCT4, and of CD147/BASIGIN, a chaperone required for MCT4 relocalization at the cytoplasmic membrane (Fig. 3*H* and Fig. S6*C*). Strikingly, *E4f1*(K14)KO mice exhibited lactic acidemia and increased level of circulating ketone bodies, a by-product of FAO (Fig. 3 *I* and *J*). Moreover, the clonogenic potential of *E4f1*KO keratinocytes was partly rescued by addition of exogenous acetate that can replenish AcCoA pools (Fig. 3*K*), confirming that the profound metabolic reprogramming of E4F1-deficient keratinocytes impinged on their biological functions.

Metabolic Reprogramming of E4F1-Deficient Keratinocytes Associates with Remodeling of the Microenvironment and Loss of Adhesion of the ESC with the Basement Membrane. In many tumors, increased lactate secretion has been linked to the remodeling of the extracellular matrix (ECM) and degradation of the basement membrane (BM) by ECM-remodeling enzymes (26). To further characterize the consequences of the metabolic reprogramming of E4F1-deficient keratinocytes, we performed histological analyses of *E4f1*(K14)KO skin. Electron microscopy analyses indicated that *E4f1* inactivation in basal keratinocytes resulted in disorganization of the BM, which appeared either diffused with thinner lamina densa or focally disrupted (Fig. S7*A*). Alterations of the BM in *E4f1*KO skin was confirmed upon staining of skin sections by the Gomori reticulin method, which stains the argyrophilic (silver staining) fibrous structures present in the BM (Fig. S7*B*). Immunostaining of skin samples prepared from *E4f1(K14)*KO mice with anti-laminin V antibody showed that the expression pattern of this essential component of the BM was diffused and focally discontinuous in *E4f1*KO skin sections compared with its defined and continuous pattern in control samples (Fig. 4*A*). This defect also correlated with an abnormal expression pattern of integrin β4 (Itgβ4). In areas showing broad disruption of the BM, Itgβ4 expression was not restricted to the basal pole of keratinocytes but was also detected at the apical or lateral sides of both basal and suprabasal keratinocytes (Fig. 4*A*). Remodeling of the ECM within the dermal compartment was also evidenced by picro-Sirius red staining of collagen fibers on skin sections prepared from tam-treated *E4f1*(*K14*)KO mice (Fig. S7*C*). These results led us to investigate whether the massive remodeling of the ECM and alterations of the BM observed upon *E4f1* inactivation resulted from increased activity of ECM-remodeling enzymes. Increased matrix metallopeptidase 9 (MMP9) and cathepsin activities were detected by gelatin-zymography in protein extracts prepared from total skin samples of tam-treated *E4f1*(*K14*)KO mice (Fig. 4*B* and Fig. S7*D*). Moreover, increased MMP2, MMP9, and cathepsin activities were also evidenced in the culture medium of *E4f1*KO primary keratinocytes (Fig. 4 *C* and *D*). Addition of the LDH-inhibitor oxamate in the culture medium decreased cathepsin activities, confirming that their induction resulted from the metabolic reprogramming of these cells (Fig. 4*D*). Moreover, stable expression of ectopic TIMP1, a broad MMP inhibitor, in feeder cells partly rescued the clonogenic potential of *E4f1*KO ESC (Fig. 4*E*). Improved clonogenicity of E4F1-deficient ESC was also observed upon incubation with GM6001, a pharmacological MMP inhibitor with broad spectrum (Fig. 4*F*). Taken together, these data indicate that the induction of ECM remodeling enzymes in E4F1-deficient keratinocytes is a consequence of their metabolic reprogramming and impinges on their clonogenic potential.

Based on these results, we hypothesized that the observed disruption of the BM impacted on the maintenance of ESC within their normal microenvironment, leading to the definitive exhaustion of the ESC pool. To test this hypothesis, we analyzed EdU$^+$ LRCs on skin sections prepared from *E4f1*(*K14*)KO mice or control littermates 2 wk after tam administration and evaluated their localization within the epidermis. The same skin sections were also processed to assess MCT4 expression as a surrogate marker of the metabolic reprogramming of *E4f1*KO

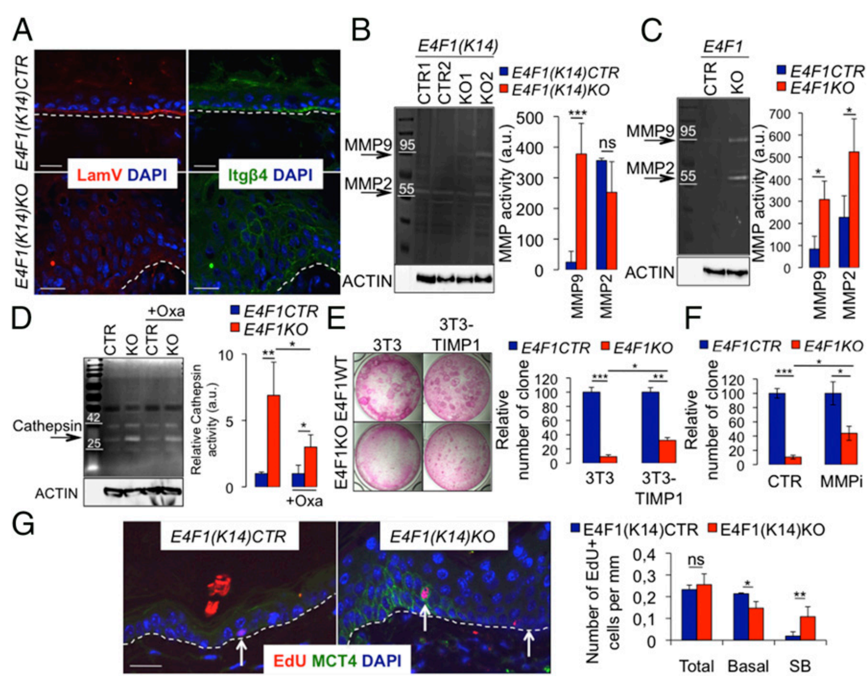

Fig. 4. *E4f1* inactivation in basal keratinocytes results in alterations of the BM, remodeling of the ECM and ESC mislocalization. (*A*) IF analysis of Laminin V (LamV, red) and Intβ4 (green) expression in skin sections prepared from *E4f1*(*K14*)KO and CTR mice, 2 wk after tam administration. Sections were counterstained with DAPI (blue). (Scale bars, 50 μm.) (*B*, *Left*) Representative zymogel analysis of MMP activities in protein extracts prepared from skin samples of *E4f1*(*K14*)KO and CTR mice, 2 wk after tam administration. For normalization, β-actin immunoblotting was performed on the same protein extracts. (*Right*) Quantification of MMP2 and MMP9 activities (mean ± SEM, $n = 5$ animals per group). (*C*, *Left*) MMP activities measured by zymography in conditioned media (CM) from *E4f1KO* or CTR cultured primary keratinocytes. For normalization, β-actin expression was analyzed by immunoblotting in protein extracts prepared from the same cells. (*Right*) Quantification of MMP2 and MMP9 activities (mean ± SEM, $n = 4$). (*D*, *Left*) Cathepsin activities measured by zymogel in CM from *E4f1KO* or CTR primary keratinocytes cultured in the presence or absence of oxamate. (*Right*) Quantification of cathepsin activities (mean ± SEM, $n = 3$). (*E*) Clonogenic assays performed with *E4f1KO* and CTR primary keratinocytes in presence of feeders transduced with empty or TIMP1-encoding retroviruses (mean ± SEM; $n = 9$). (*F*) Clonogenic assays performed with *E4f1KO* and CTR primary keratinocytes in presence or absence or the MMP-inhibitor GM6001 (mean ± SEM; $n = 6$). (*G*) Mislocalization of *E4f1KO* ESC. LRCs were identified by IF on skin sections prepared from *E4f1*(*K14*)KO and CTR mice, 2 wk after tam administration. MCT4 costaining was performed to identify metabolically reprogrammed cells. Sections were counterstained with DAPI. (Scale bar, 30 μm.) Arrows indicate EdU$^+$ LRCs. Histobars represent the total number of EdU$^+$ LRCs per millimeter of epidermis and their respective localization in the basal or suprabasal (SB) layers (mean ± SEM, $n = 4$ animals per group). $^{***}P < 0.001$; $^{**}P < 0.01$; $^{*}P < 0.05$; ns, not significant.

keratinocytes. Two weeks after tam administration, *E4f1*KO epidermis displayed approximately the same number of EdU^+ LRCs than control epidermis (0.25 ± 0.05 vs. 0.23 ± 0.02 per millimeter, respectively). However, the number of *E4f1*KO LRCs in a suprabasal position was significantly increased compared with LRCs of control epidermis that remained, as expected, in the basal layer (suprabasal: 0.1 ± 0.04 vs. 0.01 ± 0.01; basal: 0.14 ± 0.03 vs. 0.21 ± 0.003 per millimeter, respectively) (Fig. 4*G*). Interestingly, this atypical feature of *E4f1*KO LRCs was particularly evident within focal epidermal lesions exhibiting MCT4 positivity, whereas LRCs remained in contact with the BM in the adjacent $MCT4^-$ areas of the same epidermis (Fig. 4*G*). Five weeks after tam administration, the number of LRC diminished in *E4f1*KO epidermis, confirming that *E4f1* inactivation finally ended in the exhaustion of the ESC pool (Fig. 1*D*). Thus, these data show that the metabolic reprogramming triggered by *E4f1* inactivation in basal keratinocytes associates with the remodeling of their microenvironment and alterations of the BM, leading to the loss of attachment of the ESC within their normal niche and their definitive loss.

DLAT Is a Central Component of the E4F1-Regulated Metabolic Program in Basal Keratinocytes. Because *Dlat* appeared as one of the most deregulated E4F1 target gene in the epidermis of tam-treated *E4f1*(*K14*)KO animals, we evaluated the consequences of shRNA-mediated depletion of *Dlat* in primary keratinocytes. Lentiviral-mediated delivery of shRNAs targeting *Dlat* in populations of primary murine keratinocytes led to an expected decrease of DLAT protein level and PDH activity (Fig. 5*A* and Fig. S8*A*) and induced phenotypes that were reminiscent of those observed in *E4f1*KO keratinocytes. Thus, DLAT depletion in primary keratinocytes resulted in their metabolic reprogramming, as illustrated by increased MCT4 expression, and increased MMP2, MMP9, and cathepsin activities (Fig. 5 *B* and *C* and Fig. S8 *B* and *C*). Furthermore, similarly to E4F1-deficient ESC, DLAT-depleted keratinocytes also displayed an alteration of their clonogenic potential (Fig. 5*D*). Taken together, these data strengthen the role of DLAT as a central component of E4F1-regulated metabolic program in primary keratinocytes.

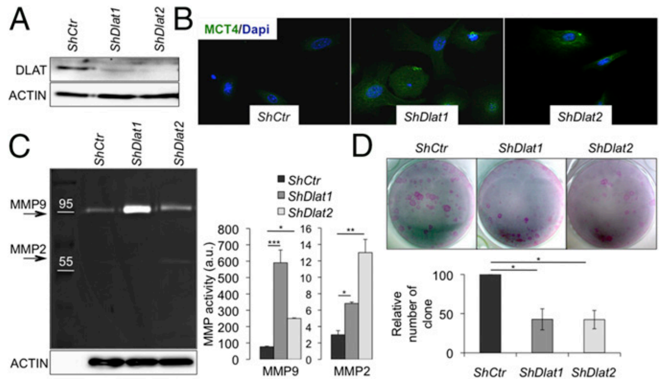

Fig. 5. DLAT depletion in primary murine keratinocytes results in their metabolic reprogramming, increased MMP activity and ESC defects. (*A*) DLAT and ACTIN (loading control) expression determined by immunoblotting in total protein extracts prepared from murine primary keratinocytes transduced with lentiviruses encoding control or *Dlat* ShRNAs. (*B*) IF analysis of MCT4 expression in murine primary keratinocytes expressing control or *Dlat* ShRNAs. (Magnification: 40×.) (*C*, *Left*) MMP activities measured by zymogel in CM from primary keratinocytes expressing control or *Dlat* ShRNAs. (*Right*) Quantification of MMP2 and MMP9 activities (mean ± SEM, $n = 3$). (*D*) Clonogenic assays performed with primary murine keratinocytes expressing control or *Dlat* ShRNAs (mean value ± SEM; $n = 5$).

Discussion

Our analyses performed in different mouse models where *E4f1* was genetically inactivated in the basal or the spinous layers of the epidermis show that the complex skin phenotypes observed upon *E4f1* inactivation originate from defects in basal keratinocytes. Our results indicate that E4F1 deficiency in these cells leads to a metabolic reprogramming of keratinocytes that affects skin homeostasis and ended in the definitive exhaustion of the ESC pool. We found that this metabolic shift, which includes the redirection of the glycolytic flux toward lactate production, is a direct consequence of PDH deficiency. Moreover, our data identify DLAT, the E2 subunit of the PDC, as an essential component of this metabolic program regulated by E4F1 in keratinocytes.

Whether E4F1-mediated control of the PDC in keratinocytes is clinically relevant remains to be determined. It is worth noting, however, that a homozygous nonsynonymous mutation in the coding region of the *E4f1* gene has been recently identified in a patient presenting clinical symptoms resembling those of Leigh syndrome patients (27). Although skin abnormalities have been reported only in some Leigh syndrome patients (28), they are part of the broad spectrum of clinical manifestations that are commonly observed in several mitochondrial disorders (29). Further investigations are necessary to evalutate whether E4F1-mediated control of mitochondrial activities, which likely extend beyond the control of the PDC, contribute to the skin manifestations observed in these patients.

Another pathological situation that has been associated with changes in PDH activity is cancer. Interestingly, the metabolic rewiring of *E4f1*KO keratinocytes is reminiscent of the one observed in many cancer cells that display increased aerobic glycolysis, even in high oxygen conditions, an effect known as the Warburg effect. It is well established that PDH deregulation in cancer cells can result from posttranslational modifications of PDC subunits by inhibitory kinases (PDKs), activating phosphatases (PDPs), or the lipoamidase SIRT4 (30, 31). We failed to detect deregulation of *Pdks* and *Pdps* mRNA levels in *E4f1*KO keratinocytes, and our data rather support the notion that transcriptional control of *Dlat* is the main mechanism by which E4F1 controls PDH activity in normal epidermal cells. It remains to be seen whether E4F1-mediated control of *Dlat* is an alternative regulatory mechanism of the PDC in skin cancer cells. Nevertheless, our data clearly show that the control of PDH activity by E4F1 in basal keratinocytes is essential for normal skin homeostasis.

Interestingly, as with cancer cells, we show that the metabolic reprogramming of *E4f1*KO basal keratinocytes results in increased activity of ECM-remodeling enzymes, including MMPs and cathepsins. The exact molecular mechanism by which increased glycolysis activates MMP activity in cancer cells remains controversial. Previous studies have suggested that the MCT-chaperone CD147/BASIGIN increases MMP activity through a yet undefined mechanism (32). However, recent data contradict this working model (33). Whatever the mechanism, the high glycolytic profile and increased activity of tissue-remodeling enzymes of fully transformed cells have been associated with their increased migratory and invasive properties that contribute to metastatic dissemination. Our data show that the metabolic reprogramming of normal *E4f1*KO keratinocytes recapitulates some features of cancer cells, including their ability to induce the focal degradation of the basement membrane and to remodel their microenvironment. Here, we show that these alterations impact on ESC maintenance within their niche, leading to their mechanical elimination and ending in the complete exhaustion of the ESC pool. Interestingly, we previously reported that the ability of E4F1 to control the Bmi1–ARF–p53 pathway partly contributes to ESC self-renewal (7). These data raise interesting questions regarding the connection between the metabolic reprogramming of E4F1-deficient keratinocytes and the deregulation of the p53 pathway in these cells. The potential crosstalk between PDH activity and the control of the p53 pathway is a promising hypothesis that warrants further investigation.

It was recently proposed that basal keratinocytes rely more on glycolysis to sustain their energetic demand than their differentiated progeny in which mitochondrial-reactive oxygen species trigger epidermal differentiation through Notch and β-catenin signaling (6). Our data do not necessarily contradict this model, but provide clear evidence that when glycolysis is further increased in basal keratinocytes, such as in E4F1-deficient cells, this profoundly alters epidermal homeostasis and ESC maintenance. Our results also question the mechanisms leading to the inhibition of keratinocyte differentiation observed in *E4f1*KO epidermis.

Altogether our results identify E4F1 as an essential regulator of the metabolic status of basal keratinocytes and stress the importance of a tight control of the PDH activity for epidermal homeostasis.

Materials and Methods

Generation of Mouse Models and Experimental Treatment. Generation of *E4f1* KO and *E4f1* cKO mice was previously described (7, 19). These mice were intercrossed with K14CreER (20) or K10CreER^{T2} mice to generate experimental groups (*E4f1*$^{+/flox}$; *K14CreER*, *E4f1*$^{-/flox}$; *K14CreER*, *E4f1*$^{+/flox}$; *K10CreER*^{T2}, and *E4f1*$^{-/flox}$; *K14CreER*^{T2} [referred as to *E4F1*(*K14*)CTR, *E4F1*(*K14*)KO, *E4F1*(*K10*)CTR, *E4F1*(*K10*)KO, respectively]. Compound mice were maintained on a mixed genetic background (129Sv/J/DBA/C57BL/6) and housed in a pathogen-free barrier facility. Cre-mediated recombination of the *E4f1*^{flox} allele was induced by topical applications of tamoxifen (Sigma; diluted in ethanol, 2 mg/d for 4 consecutive days) on shaved back or tail skin of 8- to 12-wk-old animals. Experiments were approved by the regional ethics committee for animal welfare (Comité éthique pour l'expérimentation animale du Languedoc Roussillon, protocol 12068). Oligonucleotides used for genotyping these animals are provided as in *SI Materials and Methods*.

Histology, IHC, and Immunolabeling of Skin Sections. IHC and immunolabeling of skin sections were performed as previously described (7) using the following antibodies: anti-DLAT (sc-32925 Santa Cruz), MCT4 (sc-50329 Santa Cruz), BASIGIN (G-19 sc-9757, Santa Cruz), Laminin V (generous gift from C. Feral's laboratory, University of Nice, Nice, France), Intβ4 (553745 BD Pharmingen), K14 (PRB-155P (Covance), K10 (PRB-159P Covance), Involucrin (sc-15230 Santa Cruz).

Culture of Primary Keratinocytes. Murine primary keratinocytes were isolated from newborn skin as previously described (7) and grown in calcium-free Eagle's MEM (Bio-Whittaker; Lonza) supplemented with 8% (vol/vol) calcium-free FBS (Sigma). Cre-mediated recombination was achieved by adding 4-hydroxy Tamoxifen (4OHT, Sigma; 1 μM final) to the culture medium.

Lactate, Ketone Bodies, and PDH Activity Measurement. Lactate and ketone bodies concentration were measured from tail blood samples using a lactometer (EKF Diagnostics) and β-ketone strips (Optium, Abbott). PDH activity was measured with PDH Enzyme Activity Dipstick Assay Kit (Abcam) and PDH Activity Colorimetric Assay kit (Biovision) according to the manufacturers' recommendations.

Statistic Analyses. The unpaired Student's *t* test was used in all analyses. Statistical significance was expressed as follows: $*P < 0.05$, $**P < 0.01$, $***P < 0.001$.

ACKNOWLEDGMENTS. We thank all members of the animal, imaging, cytometry, and histology facilities (Unité Mixte de Service, UMS3426 Montpellier BioCampus) for technical help; and C. Blanpain's and P. Coopman's laboratories for advices with FACS analyses and gel zymography. This work was supported by the Agence Nationale pour la Recherche (ANR), the INSERM Avenir Program, the Institut National du Cancer, the Site de Recherche Intégrée sur le Cancer (Grant "INCa-DGOS-INSERM 6045), the Association pour la Lutte Contre le Cancer (ARC), and a European Regional Development Fund (ERDF)-Languedoc Roussillon grant (Transportome) (to M.S.). B.S. is funded by the Laboratory of Excellence from Genome and Epigenome to Molecular Medecine (Labex EpiGenMed, a program of the French National Research Agency, ANR-10-LABX-12-01).

PHYSIOLOGY

1. Rishikaysh P, et al. (2014) Signaling involved in hair follicle morphogenesis and development. *Int J Mol Sci* 15(1):1647–1670.
2. Hsu Y-C, Li L, Fuchs E (2014) Emerging interactions between skin stem cells and their niches. *Nat Med* 20(8):847–856.
3. Tadeu AMB, Horsley V (2014) Epithelial Stem Cells in Adult Skin. *Curr Top Dev Biol* 107:109–131.
4. Liu J, et al. (2009) Bmi1 regulates mitochondrial function and the DNA damage response pathway. *Nature* 459(7245):387–392.
5. Castilho RM, Squarize CH, Chodosh LA, Williams BO, Gutkind JS (2009) mTOR mediates Wnt-induced epidermal stem cell exhaustion and aging. *Cell Stem Cell* 5(3):279–289.
6. Hamanaka RB, et al. (2013) Mitochondrial reactive oxygen species promote epidermal differentiation and hair follicle development. *Sci Signal* 6(261):ra8.
7. Lacroix M, et al. (2010) Transcription factor E4F1 is essential for epidermal stem cell maintenance and skin homeostasis. *Proc Natl Acad Sci USA* 107(49):21076–21081.
8. Raychaudhuri P, Rooney R, Nevins JR (1987) Identification of an E1A-inducible cellular factor that interacts with regulatory sequences within the adenovirus E4 promoter. *EMBO J* 6(13):4073–4081.
9. Rooney RJ, Raychaudhuri P, Nevins JR (1990) E4F and ATF, two transcription factors that recognize the same site, can be distinguished both physically and functionally: a role for E4F in E1A trans activation. *Mol Cell Biol* 10(10):5138–5149.
10. Fajas L, et al. (2001) Cyclin A is a mediator of p120E4F-dependent cell cycle arrest in G1. *Mol Cell Biol* 21(8):2956–2966.
11. Sandy P, et al. (2000) p53 is involved in the p120E4F-mediated growth arrest. *Oncogene* 19(2):188–199.
12. Le Cam L, et al. (2006) E4F1 is an atypical ubiquitin ligase that modulates p53 effector functions independently of degradation. *Cell* 127(4):775–788.
13. Chagraoui J, et al. (2006) E4F1: A novel candidate factor for mediating BMI1 function in primitive hematopoietic cells. *Genes Dev* 20(15):2110–2120.
14. Nojima J, et al. (2010) Dual roles of Smad proteins in the conversion from myoblasts to osteoblastic cells by bone morphogenetic proteins. *J Biol Chem* 285(20):15577–15586.
15. Fenton SL, et al. (2004) Identification of the E1A-regulated transcription factor p120 E4F as an interacting partner of the RASSF1A candidate tumor suppressor gene. *Cancer Res* 64(1):102–107.
16. Tessari MA, et al. (2003) Transcriptional activation of the cyclin A gene by the architectural transcription factor HMGA2. *Mol Cell Biol* 23(24):9104–9116.
17. Hatchi E, et al. (2011) E4F1 deficiency results in oxidative stress-mediated cell death of leukemic cells. *J Exp Med* 208(7):1403–1417.
18. Rodier G, et al. (2015) The transcription factor E4F1 coordinates CHK1-dependent checkpoint and mitochondrial functions. *Cell Reports* 11(2):220–233.
19. Le Cam L, Lacroix M, Ciemerych MA, Sardet C, Sicinski P (2004) The E4F protein is required for mitotic progression during embryonic cell cycles. *Mol Cell Biol* 24(14):6467–6475.
20. Vasioukhin V, Degenstein L, Wise B, Fuchs E (1999) The magical touch: Genome targeting in epidermal stem cells induced by tamoxifen application to mouse skin. *Proc Natl Acad Sci USA* 96(15):8551–8556.
21. Braun KM, et al. (2003) Manipulation of stem cell proliferation and lineage commitment: Visualisation of label-retaining cells in wholemounts of mouse epidermis. *Development* 130(21):5241–5255.
22. Lacroix M, et al. (2016) E4F1 controls a transcriptional program essential for pyruvate dehydrongenase activity. *Proc Natl Acad Sci USA* 113:10998–11003.
23. Herzig S, et al. (2012) Identification and functional expression of the mitochondrial pyruvate carrier. *Science* 337(6090):93–96.
24. Bricker DK, et al. (2012) A mitochondrial pyruvate carrier required for pyruvate uptake in yeast, *Drosophila*, and humans. *Science* 337(6090):96–100.
25. Lindhurst MJ, et al. (2006) Knockout of Slc25a19 causes mitochondrial thiamine pyrophosphate depletion, embryonic lethality, CNS malformations, and anemia. *Proc Natl Acad Sci USA* 103(43):15927–15932.
26. Zucker S, et al. (2001) Tumorigenic potential of extracellular matrix metalloproteinase inducer. *Am J Pathol* 158(6):1921–1928.
27. Legati A, et al. (2016) New genes and pathomechanisms in mitochondrial disorders unraveled by NGS technologies. *Biochim Biophys Acta BBABioenerg* 1857(8): 1326–1335.
28. Bodemer C, et al. (1999) Hair and skin disorders as signs of mitochondrial disease. *Pediatrics* 103(2):428–433.
29. Feichtinger RG, Sperl W, Bauer JW, Kofler B (2014) Mitochondrial dysfunction: A neglected component of skin diseases. *Exp Dermatol* 23(9):607–614.
30. Patel MS, Korotchkina LG (2006) Regulation of the pyruvate dehydrogenase complex. *Biochem Soc Trans* 34(Pt 2):217–222.
31. Mathias RA, et al. (2014) Sirtuin 4 is a lipoamidase regulating pyruvate dehydrogenase complex activity. *Cell* 159(7):1615–1625.
32. Biswas C, et al. (1995) The human tumor cell-derived collagenase stimulatory factor (renamed EMMPRIN) is a member of the immunoglobulin superfamily. *Cancer Res* 55(2):434–439.
33. Marchiq I, et al. (2015) Knock out of the BASIGIN/CD147 chaperone of lactate/H+ symporters disproves its pro-tumour action via extracellular matrix metalloproteases (MMPs) induction. *Oncotarget* 6(28):24636–24648.
34. Manel N, et al. (2003) The ubiquitous glucose transporter GLUT-1 is a receptor for HTLV. *Cell* 115(4):449–459.
35. Dumas JE, Platt MO (2013) Systematic optimization of multiplex zymography protocol to detect active cathepsins K, L, S, and V in healthy and diseased tissue: Compromise among limits of detection, reduced time, and resources. *Mol Biotechnol* 54(3):1038–1047.